Communications

Beyond the Gamma Band: The Role of High-Frequency Features in Movement Classification

Kai J. Miller*, Pradeep Shenoy, Marcel den Nijs, Larry B. Sorensen, Rajesh P. N. Rao, and Jeffrey G. Ojemann

***Abstract*—Electrocorticographic spectral changes during movement show a behavioral inflection in the classic gamma band (30–70 Hz). We quantify this inflection and demonstrate that it limits classification accuracy. We call for the designation of a functionally defined band above it, which we denote the χ-band.**

***Index Terms*—Chi (χ) band, electrocorticographic spectrum.**

I. Introduction

Several current brain–computer interfaces (BCIs) using electrocorticographic (ECoG) arrays rely upon changes in the power of specific spectral bands associated with actual or imagined motor movement [4]–[7], [14], [18], [19]. The α (8–12) and β (14–25 Hz, also known as μ [12]) bands have been associated in the BCI literature with characteristic decreases in power with movement compared with rest over a range of motor tasks. Recent results have demonstrated that cortical spectral changes during movement imagery mimic those of actual movement. The γ range (>30 Hz) has been reported to show a corresponding power increase [2], [3], [12], [14]. In a previous paper, we hypothesized the existence of two complementary processes: one is the dissolution of power in band-specific peaks in the classic electroencephalography (EEG) frequency range (up to ~50 Hz) with movement [event-related desynchronization—entity relationship diagram (ERD) [Fig. 1(A)], [12]. The other is a power-law like broad spectral increase across all frequencies [Fig. 1(B)] that is most cleanly observed at high frequencies because it is masked by an ERD at low frequencies [Fig. 1(C)]. The superposition of these two phenomena produces an intersection point between power spectra for movement and rest inside the classic gamma range. We denote this the "primary junction" (J_0) [9]. In a previous paper, we demonstrated how the integrated power in a high-frequency band, characteristically above J_0, could capture the broad spectral increase (χ-index), and allows functional mapping of the brain in real time [8]. In this paper, we quantify the frequency values for J_0, and show how they influence binary classification accuracy between both movement and rest, and between two different types of movement. The choice of a frequency range above this, χ, will be shown to be the best for classification.

Manuscript received July 18, 2007; revised October 16, 2007. This work was supported in part by the National Science Foundation (NSF) under Grant 0622252 and Grant 0130705, in part by the National Institutes of Health (NIH) under Grant T32-NS07144, and in part by the Poncin Foundation. *Asterisk indicates corresponding author.*

*K. J. Miller is with the Department of Physics, University of Washington, Seattle, WA 98195 USA (e-mail: kjmiller@u.washington.edu).

P. Shenoy and R. P. N. Rao are with the Department of Computer Science and Engineering, University of Washington, Seattle, WA 98105 USA (e-mail: pshenoy@cs.washington.edu; rao@cs.washington.edu).

M. den Nijs, L. B. Sorensen, and are with the Department of Physics, University of Washington, Seattle, WA 98195 USA (e-mail: dennijs@phys.washington.edu; seattle@u.washington.edu).

J. G. Ojemann is with the Department of Neurological Surgery, University of Washington, Seattle, WA 98105 USA (e-mail: jojemann@u.washington.edu).

Color versions of one or more of the figures in this paper are available online at http://ieeexplore.ieee.org.

Digital Object Identifier 10.1109/TBME.2008.918569

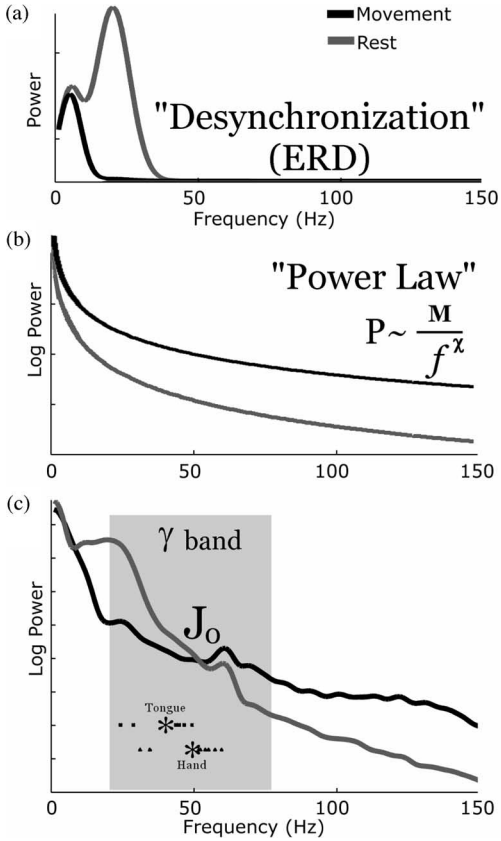

Fig. 1. Schematic illustrations of the two types of processes which create a junction in the power spectrum. (a) Decoherence of discrete peaks in the power spectrum with movement (ERD). (b) Power-law like power spectrum that shifts upward with movement. It is most easily observed at high frequencies because it is masked by peaked ERD at low frequencies. (c) Example of an actual spectrum that demonstrates the spectral shift between hand movement and rest for the most task-specific electrode (also for hand movement) for subject 5. The superposition of the phenomena in (a) and (b) produces an intersection (J_0) in the power spectrum in the classic gamma range (shown shaded). The squares and triangles below the curves in the shaded region indicate the individual values of J_0 for tongue and hand, respectively. Asterisks indicate the mean values across subjects; for hand movement, $J_0 = 48 \pm 9$ Hz (mean $\pm$ SD) (range 32–57 Hz), for tongue movement, $J_0 = 40 \pm 8$ Hz (range 26–48 Hz). The individual values for each subject can be found in Table I.

II. Methods

Eight patients (Table I) at the University of Washington Regional Epilepsy Center (Seattle, WA) were implanted with subdural platinum electrode arrays (AdTech, Racine, WI) for 7–10 days monitoring prior to seizure focus resection, during which they participated in this motor task study. Data were sampled in parallel with the clinical recording system using Synamps2 amplifiers (Neuroscan, El Paso, TX) recording at 1000 Hz, with a bandpass filter from 0.15 to 200 Hz. A scalp or subdural electrode was used for reference. Electrode locations in Talairach atlas coordinates [16] were characterized from standard X-rays using the "location on cortex (LOC) package" [11]. Using the BCI2000 software [13], subjects were presented with visual stimuli instructing them to perform hand or tongue movements for 3-s-long intervals; 30 intervals of each movement kind were presented in random order. Movement intervals were interspersed with 3-s-long rest

0018-9294/$25.00 © 2008 IEEE

TABLE I
SUBJECT DESCRIPTIONS

Subject	Age	Sex	Hand	Cognitive Capacity	Grid Location	Seizure Focus	J_0 Tongue	J_0 Hand
1	21	M	R	Borderline (IQ - 76)	R Frontal-temporal	R Frontal	26	50.5
2	18	F	R	Normal	L Frontal	L Frontal	30	55
3	25	M	R	Normal	L Temporal-parietal	L Temporal	XX	50
4	38	M	R	Borderline (IQ - 70)	R Frontal	R Frontal	44	35
5	48	M	R	Borderline (IQ - 82)	R Temporal-parietal-occipital	R Temporal-occipital	48	57
6	39	F	R	Normal	R Frontal	R Frontal	43	52
7	32	M	R	Normal	L Frontal-temporal-parietal	L Temporal	43	53
8	27	F	R	Normal	L Frontal-parietal	L Frontal	45.5	32

Descriptions of each of the eight subjects: R: right; L: left; M: male; F: female; IQ: intelligence quotient. "J_0 Tongue" denotes the primary junction for tongue movement and "J_0 Hand" denotes the primary junction for hand movement, in Hertz. Subject three did not perform a tongue task, and "XX" denotes this. The J_0 values are also shown in the lower left shaded region of Fig. 1. The mean value ($\pm$ SD) of J_0 for hand is 48 $\pm$ 9 Hz, and tongue is 40 $\pm$ 8 Hz.

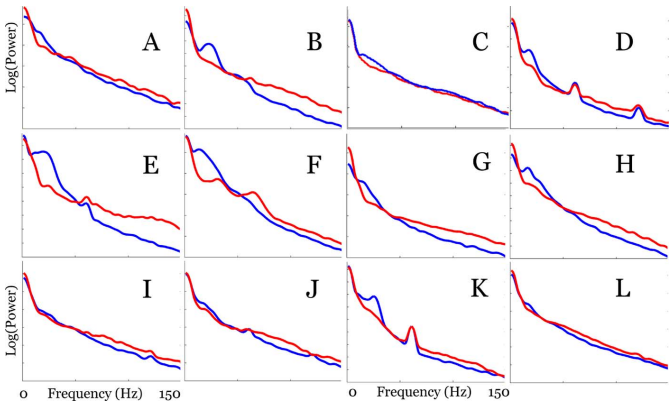

Fig. 2. Individual traces for movement versus rest to demonstrate the junction of spectra. The axes of each task are the same as in Fig. 2. Insets (A)–(H) compare hand movements (dark) to rest intervals (light) for subjects 1–8, respectively (Table I) Insets (I), (J) demonstrate the shift for tongue movement (dark) compared to rest intervals (light) for subjects 1, 4, 5, and 8, respectively. The amount of contamination from 60 and 120 Hz is variable, and can be seen in prominent peaks throughout.

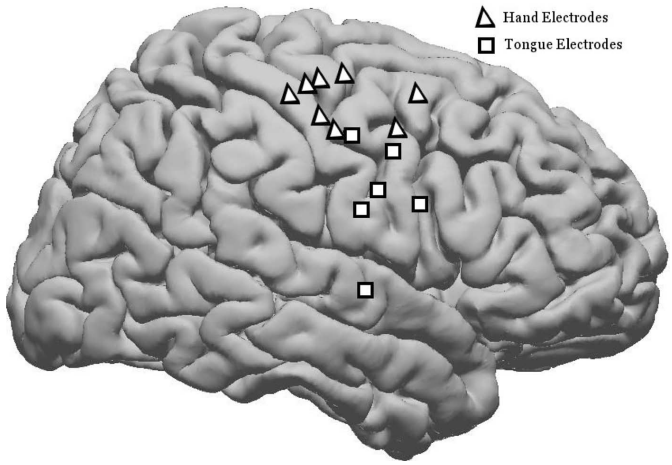

Fig. 3. This figure shows the relevant electrode locations identified for hand and tongue movement, using the LOC package [11]. Triangles denote hand areas and squares denote tongue areas. The areas found naively using the combination of an 8–32 Hz spectral decrease and a 76–100 Hz increase fall roughly in classic hand and tongue areas. Our mean position of the most task-specific electrodes were $y = -15 \pm 11$ mm (mean $\pm$ SD) and $z = 50 \pm 6$ mm for hand movement and $y = -5 \pm 6$ mm and $z = 25 \pm 14$ mm for tongue movement, in Talairach coordinates [18].

periods. During the movement intervals, the subjects would clench and unclench their hand (contra-lateral to electrode array) three to six times, or periodically extrude their tongue three to six times.

The data were notch filtered for 60, 120, and 180 Hz to eliminate line noise, using a third-order Butterworth filter. We rereferenced the data with respect to the common average, and computed the fast Fourier transform (FFT) for the t = 1–2.5 s interval from each t = 0–3 s epoch (a subinterval was used because of jitter in behavioral response). The data from these epochs were transformed using overlapping 0.256 s (256 sample) windows with 0.1 s step sizes between them. A Hann window was imposed on each data window to attenuate edge effects. Spectral coefficients were normalized with respect to a baseline period. For classification accuracy, we looked at a gamut of ranges: the classic ranges of low α (7–12 Hz), high α (10–13 Hz), β (14–25), low γ (26–35Hz), high γ (36–70 Hz) [12], as well as the higher frequency power–law range, χ (76–150 Hz, [9]). In this study, the upper limit of 150 Hz for χ was determined based upon the roll-off frequency of the built-in amplifier filter.

We identified the statistically most specific electrodes for each task by taking the maximum product of the square of cross-correlation coefficients between each movement type and rest for a low (8–32 Hz) band and a high (76–100 Hz) band [10], and identified the frequency of the primary junction (J_0) between movement and rest spectra across the entire task. In cases of multiple crossings related to noise, we took the mean value of the cross-over frequencies [Fig. 2(C) and (G)–(J)].

We measured the total integrated power $P_b(e;t,n_t)$ for each electrode "e," where "n_t" is an interval of task type "t" (t can be hand, tongue, or rest). Next, we tested how well a particular frequency range "b" (b = high- and low- α, β, high- and low- γ, χ) could be used to distinguish between the tasks. We used the library for support vector machine (LIBSVM) implementation [1] of a linear SVM classifier [17], to make pairwise class divisions between hand, tongue, and rest data, using the projection vector $P_b(e;t,n_t)$ with sixfold nested cross-validation.

III. RESULTS

The locations of each subject's most significant electrodes were in the region of sensorimotor cortex (Fig. 3). The primary junction, J_0, across these task-specific electrodes was 48 $\pm$ 9 Hz (mean $\pm$ SD) (range 32–57 Hz) for hand, and 40 $\pm$ 8 Hz (range 26–48 Hz) for tongue [Fig. 1(C) and Table I]. The classification accuracy of each band across the entire electrode array tended to increase with frequency band, with the notable exception of the high-γ band, and was always highest in the χ-band (Fig. 4 and Table II). The χ-band classification accuracy was never below 83% for all individuals (with a mean of 91%) whereas the low and high γ-band mean classification rates were 74–79% for movement versus rest classification. The high γ-band was at or below the classification accuracy level of the low γ-band in both of the movement versus rest tasks, but well above the low γ-level in

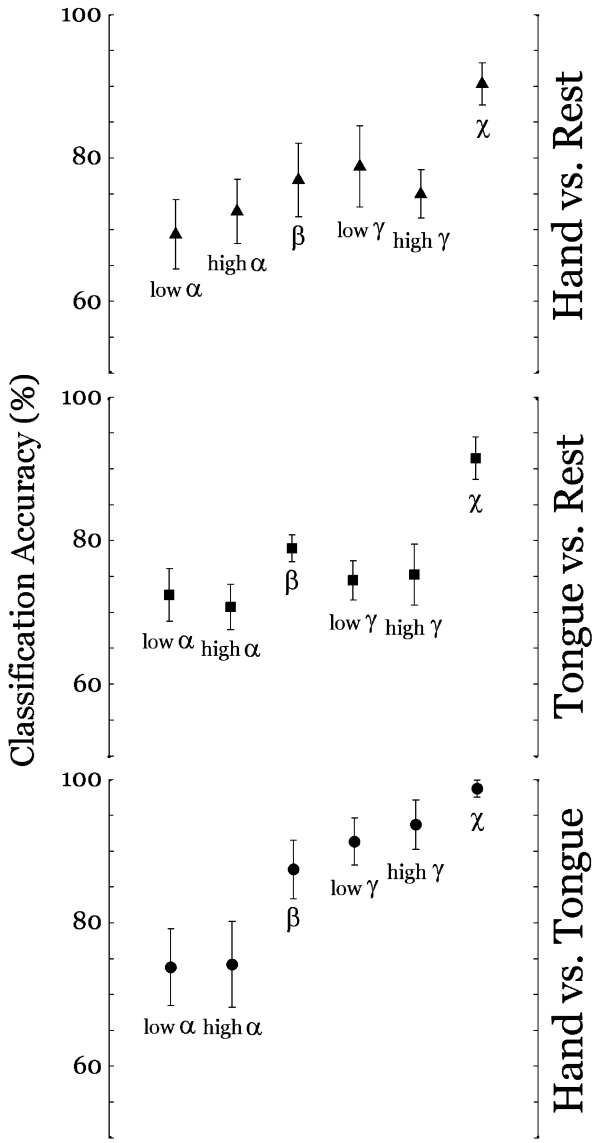

Fig. 4. Classification accuracy percentages for hand, tongue, and rest intervals using an SVM with six-fold cross-validation. Error bars indicate the standard error of the mean. The frequency ranges used for classification were low α (7–12 Hz), high α (10–13 Hz), β (14–25 Hz), low γ (26–35 Hz), high γ (36–70 Hz), and χ (76–150 Hz, chosen such that $\chi > J_0$). Note that, in the movement versus rest classifications (top two graphs), the γ ranges suffer (high in both, low in tongue versus rest). We propose that the reason which classification suffers in these, and not in the hand movement versus tongue movement comparison, is that fluctuations in ERD when shifting between rest and movement confuse classification. In the case of comparison between different types of movement, the J_0 is largely absent (due to the spatially broad nature of the ERD), and so classification in the γ bands is much better. Individual classification values for each subject, in each range, can be found in Table II.

hand versus tongue movement tasks, where the variable difference in the ERD/economic research service (ERS) compared to the rest state was no longer a factor.

IV. Discussion

Examining the most task-specific electrodes, we obtained characteristic values for a junction J_0 in the ECoG power spectra that lies in the classical gamma band (>25 Hz) and separates two characteristic movement-related phenomena: a decrease in low-frequency power and an increase in power at high frequencies. The existence of such a junction constrains the classic gamma band as a practical feature for cortical mapping or control in a BCI. We propose that this junction, which spans 25–55 Hz, is due to the superposition of two distinct phenomena: 1) the formation and dissolution of distinct spectral peaks at low frequencies (ERD/ERS [12]) and 2) shifts in a power law that extends across the entire range of frequencies (see Fig. 1). When classification accuracy was evaluated by frequency band (using all electrodes), classifiability using the high γ range was much lower for both types of movement versus rest than in a direct comparison of hand versus tongue movement. We suggest that this feature confusion near J_0 is due to fluctuations in ERD when shifting between rest (peak in the power spectrum) and movement (no peak in the power spectrum). In direct comparisons between different types of movement, the peak is largely absent (ERD is spatially broad for both cases [8]–[10]). As a result, J_0 is also largely absent, and classification using the classic gamma band improves.

Based upon our results, the optimal range for spectral-band-based features for BCIs and brain mapping (that may include resting states) uses the broad spectral power of the χ-index.

TABLE II
Classification Accuracy

A. Hand vs. Rest

Subject	J_0 Hand	low α	low α	β	low γ	high γ	χ
1	50.5	67	70	73	80	77	83
2	55	50	47	83	92	70	100
3	50	80	78	70	63	65	82
4	35	67	75	78	78	70	88
5	57	85	85	93	93	85	98
6	52	88	87	97	100	88	96
7	53	60	73	52	53	63	92
8	32	58	65	68	70	78	85
Mean		69	73	77	79	75	91

B. Tongue vs. Rest

Subject	J_0 Tongue	low α	low α	β	low γ	high γ	χ
1	26	70	60	73	83	87	90
2	30	88	75	78	67	90	98
4	44	67	62	85	73	58	87
5	48	57	70	73	83	73	82
6	43	74	84	83	79	71	94
7	43	75	73	83	68	82	88
8	45.5	77	72	77	68	85	98
Mean		73	71	79	74	78	91

C. Hand vs. Tongue

Subject	J_0H	J_0T	low α	low α	β	low γ	high γ	χ
1	51	26	83	83	93	100	100	100
2	55	30	57	55	78	83	100	100
4	35	44	55	50	78	78	78	92
5	57	48	78	75	72	100	92	100
6	52	43	94	92	97	99	96	99
7	53	43	77	85	97	88	97	100
8	32	46	72	78	97	90	98	100
Mean			74	74	87	91	94	99

Classification accuracies for hand, tongue, and rest intervals using an SVM with 6-fold cross-validation: "Subjects" column corresponds to the subjects from Table I. The J_0 columns detail the $\mathbf{J}_0$ values for hand ($\mathbf{J}_0$H in (C)) and tongue ($\mathbf{J}_0$T in (C), in HZ. The values of $\mathbf{J}_0$ are rounded in (C). Note that subject 3 did not perform a tongue movement task, and is only included in the "Hand vs. Rest" classification. These results are reproduced in Fig. 2 of the text. Note that all accuracies are percentage (%) values, and are rounded to the nearest percentage.

Acknowledgment

The authors would like to thank the staff and patients at Harborview Hospital, Seattle, WA, for their time, consideration, and effort on behalf of this research. They are also thankful to P. Loesche's writing group.

REFERENCES

[1] C.-C. Chang and C.-J. Lin. (2001, Dec.). *LIBSVM: A library for support vector machines* [Online]. Available: http://www.csie.ntu.edu.tw/cjlin/libsvm

[2] N. E. Crone *et al*., "Functional mapping of human sensorimotor cortex with electrocorticographic spectral analysis. Part II. Event-related synchronization in the gamma band," *Brain*, vol. 121, no. 12, pp. 2301–2315, 1998.

[3] N. E. Crone *et al*., "Functional mapping of human sensorimotor cortex with electrocorticographic spectral analysis. Part I. Alpha and beta event-related desynchronization," *Brain*, vol. 121, no. 12, pp. 2271–2299, 1998.

[4] E. A. Felton *et al*., "Electrocorticographically controlled brain–computer interfaces using motor and sensory imagery in patients with temporary subdural electrode implants. Report of four cases," *J. Neurosurg*., vol. 106, no. 3, pp. 495–1, 2007.

[5] N. J. Hill *et al*., "Classifying EEG and ECoG signals without subject training for fast BCI implementation: Comparison of nonparalysed and completely paralysed subjects," *IEEE Trans. Neural Syst. Rehabil. Eng*., vol. 14, no. 2, pp. 183–186, Jun. 2006.

[6] E. C. Leuthardt *et al*., "Electrocorticography-based brain computer interface—the Seattle experience," *IEEE Trans. Neural Syst. Rehabil. Eng*., vol. 14, no. 2, pp. 194–198, Jun. 2006.

[7] E. C. Leuthardt *et al*., "A brain–computer interface using electrocorticographic signals in humans," *J. Neural Eng*., vol. 1, no. 2, pp. 63–71, 2004.

[8] K. Miller, R. Rao, and J. Ojemann, "The behavioral split in the Gamma Band Neural Engineering," in *Proc. 3rd Int. IEEE/EMBS Conf. CNE 2007*, 2007, pp. 465–468.

[9] K. J. Miller *et al*., "Real-time functional brain mapping using electrocorticography," *Neuroimage*, vol. 37, no. 2, pp. 504–507, 2007.

[10] K. J. Miller *et al*., "Spectral changes in cortical surface potentials during motor movement," *J. Neurosci*., vol. 27, no. 9, pp. 2424–2432, 2007.

[11] K. J. Miller *et al*., "Cortical electrode localization from X-rays and simple mapping for electrocorticographic research: The "location on cortex" (LOC) package for MATLAB," *J. Neurosci. Methods*, vol. 162, no. 1–2, pp. 303–308, May 2007.

[12] G. Pfurtscheller and F. H. Lopes da Silva, "Event-related desynchronization," *Electroencephalography and Clinical Neurophysiology*, 1st ed. (Rev. Ser.). Amsterdam, New York: Elsevier, 1999, vol. 6, xxi, 406 p.

[13] G. Schalk *et al*., "BCI2000: A general purpose brain–computer interface (BCI) system," *IEEE Trans. Biomed. Eng*., vol. 51, no. 6, pp. 1034–1043, Jun. 2004.

[14] G. Schalk *et al*., "Two-dimensional movement control using electrocorticographic signals in humans," *J. Neural Eng*., vol. 5, no. 1, pp. 75–84, 2008.

[15] A. B. Schwartz *et al*., "Brain-controlled interfaces: Movement restoration with neural prosthetics," *Neuron*, vol. 52, no. 1, pp. 205–220, 2006.

[16] J. Talairach and P. Tournoux, *Co-planar Stereotaxic Atlas of the Human Brain: 3-Dimensional Proportional System: An Approach to Medical Cerebral Imaging*. Stuttgart, New York: Thieme; Thieme Medical, 1988, viii, 122 p.

[17] V. N. Vapnik, *The Nature of Statistical Learning Theory*. New York: Springer-Verlag, 1995, xv, 188 p.

[18] J. A. Wilson *et al*., "ECoG factors underlying multimodal control of a brain–computer interface," *IEEE Trans. Neural Syst. Rehabil. Eng*., vol. 14, no. 2, pp. 246–250, Jun. 2006.

[19] J. R. Wolpaw *et al*., "An EEG-based brain–computer interface for cursor control," *Electroencephalogr. Clin. Neurophysiol*., vol. 78, no. 3, pp. 252–259, 1991.

The Effect of Electrical Anisotropy During Magnetoacoustic Tomography With Magnetic Induction

Kaytlin Brinker* and Bradley J. Roth

***Abstract*—Magnetoacoustic tomography with magnetic induction (MAT-MI) is a technique for imaging electrical conductivity in tissue. A time-varying magnetic field induces currents that interact with a static magnetic field to produce a Lorentz force, initiating ultrasonic waves. The goal of this communication is to examine the effect of anisotropy during MAT-MI.**

***Index Terms*—Anisotropy, conductivity, imaging, magnetic induction, magnetoacoustic tomography.**

I. INTRODUCTION

Bin He and his colleagues [1]–[5] developed magnetoacoustic tomography with magnetic induction (MAT-MI), a noninvasive technique for imaging the electrical conductivity of biological tissue. The method uses two magnetic fields: one static and one changing with time. The time-varying magnetic field induces eddy currents in the tissue, and these eddy currents interact with the static magnetic field to produce a Lorentz force that initiates ultrasonic waves. The goal of the method is to deduce the conductivity distribution from the acoustic signal.

He and his coworkers analyzed MAT-MI both theoretically and experimentally. However, their analysis considered only isotropic tissue. Muscle and nerve are anisotropic (the conductivity depends on direction). Our goal is to examine the effect of anisotropy on the MAT-MI signal.

II. METHODS

Consider a uniform sheet of tissue having anisotropic conductivity, with the fiber direction parallel to the x-axis (Fig. 1). The static magnetic field is uniform and in the z direction, of strength $B_{\rm o}$. The time-dependent magnetic field $B\,(t)$ is also in the z direction, but is restricted to the region $r < R$, where r is the radial distance in cylindrical coordinates and R indicates the region where $B(t)$ is applied. It increases at a constant rate $\dot{B}$ from time zero to T, and then decreases at a rate $-\dot{B}$ from time T to $2\,T$, after which it is zero. Faraday induction results in an eddy current $\boldsymbol{J}$ that produces a Lorentz force per unit volume $\boldsymbol{F} = \boldsymbol{J} \times \boldsymbol{B}$. The pressure p obeys a wave equation, with the source term equal to the divergence of the Lorentz force [6], [7]

$$\nabla^2 p - \frac{1}{c^2}\frac{\partial^2 p}{\partial t^2} = \nabla \cdot (\boldsymbol{J} \times \boldsymbol{B}) \tag{1}$$

where c is the speed of sound in the tissue.

The electric field $\boldsymbol{E}$ in the tissue is

$$\boldsymbol{E} = -\frac{\partial \boldsymbol{A}}{\partial t} - \nabla V \tag{2}$$

Manuscript received August 22, 2007. This work was supported by the National Science Foundation through the Summer Materials Research Training (SMaRT) Program, a Research Experience for Undergraduates (REU) Site, at Oakland University, Rochester, MI, under Grant DMR-055 2779. *Asterisk indicates corresponding author*.

*K. Brinker is with the University of Michigan, Ann Arbor, MI 48109 USA (e-mail: kbrink@umich.edu).

B. J. Roth is with the Department of Physics, Oakland University, Rochester, MI 48309 USA (e-mail: roth@oakland.edu).

Digital Object Identifier 10.1109/TBME.2007.914001

0018-9294/$25.00 © 2008 IEEE